STRUCTURE OF MICROTUBULAR CRYSTALS
INDUCED BY VINBLASTINE IN VITRO

ROBERT MARANTZ and MICHAEL L. SHELANSKI. From the Department of Pathology
(Neuropathology), Albert Einstein College of Medicine, Bronx, New York 10461

INTRODUCTION

The treatment of any of a wide variety of cells with vincristine or vinblastine results in the dissolution of cytoplasmic microtubules and the formation of both 90–100 A filaments and ordered arrays of hexagonally packed, circular structures (1–4). These ordered structures have been named "microtubular crystals" (2, 3), and this nomenclature will be followed here with the awareness that conclusive evidence of true crystalline order is lacking.

Ultracentrifugal studies by Weisenberg and Timasheff (5) revealed a vinblastine-induced aggregation of purified microtubule subunit protein. Vinblastine selectively and quantitatively precipitates microtubule protein from supernatants of cell and tissue homogenates, if adequate concentrations of vinblastine and magnesium are used (6, 7).

Electron microscopic studies of vinblastine-precipitated microtubule protein were previously reported from this laboratory (8). These studies on embedded, sectioned material revealed ordered acriform arrays of ladder-like structures with "rungs" spaced approximately 300 A apart surrounding circular profiles with a diameter on the order of 360 A. On the basis of this sectioned material it was not possible to ascertain what relationship, if any, existed between the vinblastine-induced precipitated microtubule protein in vitro and the vinblastine-induced microtubular crystals seen in vivo.

The negative contrast studies which we now report demonstrate the remarkable similarity between the structures induced by vinblastine in vitro and in vivo. In addition, the three-dimensional structure of the former is clarified, and the results are extrapolated to the latter.

MATERIALS AND METHODS

Microtubule protein was purified from pig brain by using the method of Weisenberg, Borisy, and Taylor (9). The final ammonium sulfate pellet was resuspended in a 0.01 M phosphate buffer containing 0.01 M MgCl and 10^{-4} M guanosine-5'-triphosphate (phos-Mg-GTP) at pH 6.5. Protein concentration varied from 2 to 5 mg/ml. The purified protein ran as a single band on a 7.5% polyacrylamide gel electrophoresis after the samples had been denatured in 8 M urea, reduced, and alkylated as previously described (9, 12).

Crystals were grown by dialysis of microtubule protein solutions against Phos-Mg-GTP with 10^{-4} M vinblastine sulfate for periods of up to 18 hr. At the end of the dialysis a whitish precipitate was present. Previous work has demonstrated the complete precipitation of all microtubule protein and all colchicine-binding activity by this procedure (6). Suspensions of the precipitate were used for negative contrast examination with the electron microscope. Occasional samples were sonicated with a Branson sonicator (Branson Instruments, Inc., Stanford, Conn.) at settings varying from 1 to 3 for periods of up to 15 sec. The samples were immersed in an ice bath during this procedure.

Thin layers of the suspensions were applied to 400-mesh collodion–carbon-coated grids, and staining was then carried out by dropwise application of 0.3–0.5 ml of 2% uranyl acetate in deionized water. The grids were then blotted on filter paper and allowed to dry in air. Specimens were examined in Siemens 1A and Hitachi HS-8-1 electron microscopes calibrated against a carbon replica grid. Plates were measured directly on a Nikon Shadowgraph optical comparator (Nikon Inc., Instrument Div., New York).

RESULTS

The precipitate is composed of large, closely packed arrays of rings in hexagonal apposition

(Fig. 1). Smaller structures consisting of single rings or individual helical structures are also seen frequently (Fig. 2). Helices are also seen frequently at the periphery of the larger arrays and often appear to spiral out from the ringlike structures (Fig. 3).

Each ring has an inner diameter of 280 A and a wall width of 70–80 A, for a total diameter of 420–440 A (Figs. 1–3). The total wall thickness dividing two rings is 140 A with some overlap of the individual walls seen in the majority of rings studied (Fig. 2). The helices, which are studied more readily in mildly sonicated preparations (Figs. 4, 5), are wound from a strand of 70–80 A diameter, a dimension identical with that of the wall thickness of an individual ring. The distance between turns of the helix is approximately 250 A,

though considerable variation is found in this dimension.

The walls of the rings and the helical strands reveal a triple density appearance with two, light, outer bands surrounding a central, faintly cross-striated, dark band (Figs. 2, 4). At higher magnification (Fig. 6) this pattern gives the appearance of globules with an electron-opaque core. Each band in this triple density pattern is 20–30 A in width, and the center-to-center spacing of the dark electron-opaque units is 45–50 A.

The helices often appear to be a series of loops (Fig. 3) on a vertical spine rather than a corkscrew of uniform pitch. Due to the distortion inherent in the drying of material on the grids, this problem could not be further resolved. Small pieces of linearly assembled subunits were often
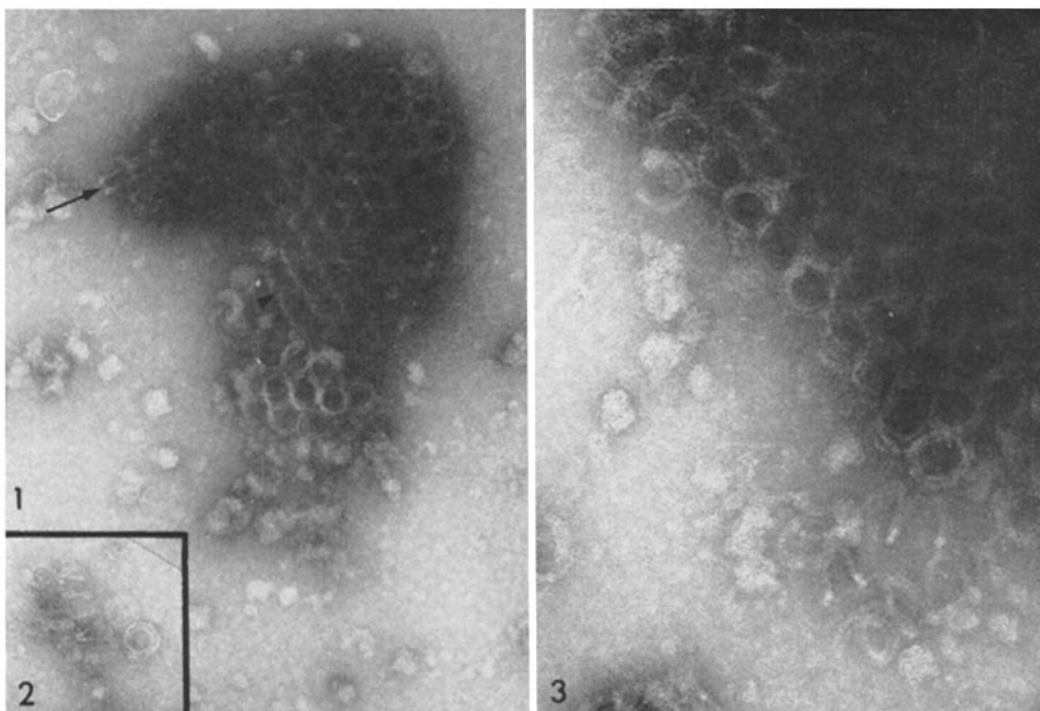
FIGURE 1 Negative contrast image of vinblastine-induced microtubule crystal. Appearance is that of hexagonally packed rings. Areas suggestive of helical structure are observed (arrows). × 100,000.

FIGURE 2 Individual rings and helix as are often seen. The adjacent rings overlap slightly at their junction. The walls of both the rings and the helix show triple density appearance with a suggestion of cross-striation. × 100,000.

FIGURE 3 Periphery of a microtubular crystal demonstrating helices arising from the regions of circular structure. In the lower portion of the figure, helices of both corkscrew and loop conformation can be seen. × 180,000.
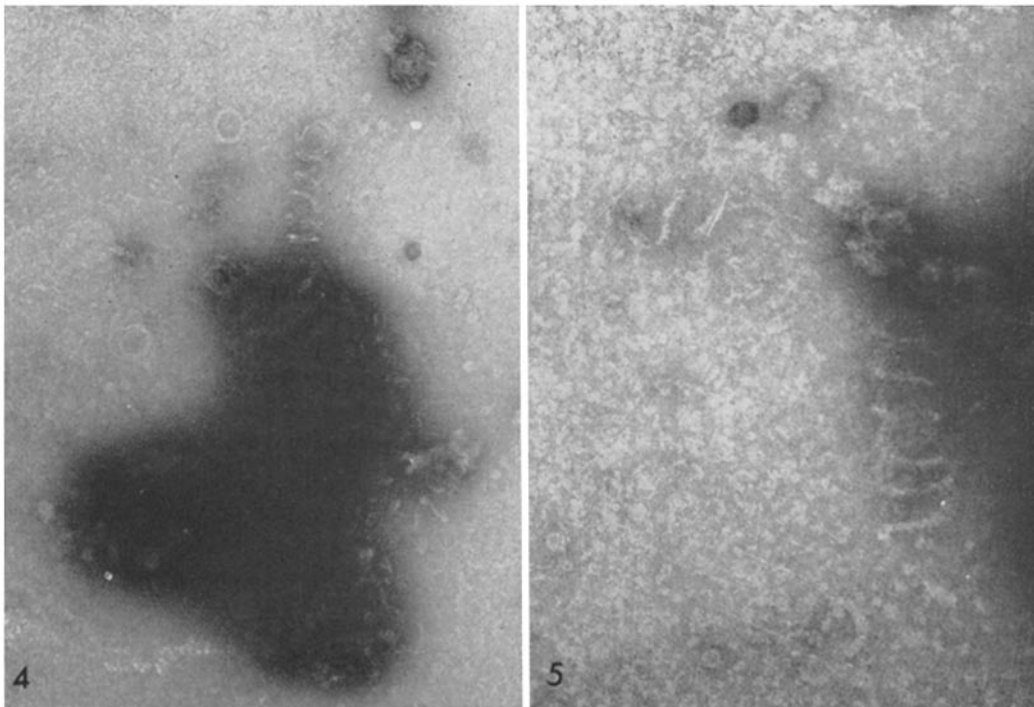
FIGURE 4 Gently sonicated crystal showing beaded or triple density appearance of strand forming the helix. Background shows isolated rings and pieces of helices. × 100,000.

FIGURE 5 High magnification view of single helix showing triple density wall. Negative contrast. ×205,000.

seen in the background of both sonicated and unsonicated preparations, but long linear filaments such as have been reported in vivo were never seen (1). Crystals were readily redissolved by dialysis against Phos-Mg-GTP. The protein could be precipitated again with identical morphology by readdition of vinblastine. Essentially similar results were obtained with vincristine. No structures were identifiable after addition of colchicine or griseofulvin at concentrations of 10^{-3} M to microtubule protein solutions. The vinblastine-induced assembly was not affected by 10^{-4} M colchicine, podophyllotoxin, or griseofulvin. The removal of GTP from the dialysis medium also has no effect on the formation of these crystals.

Preliminary studies on the binding of vinblastine to the precipitate are in progress, and a combination of colorimetric and thin-layer chromatography techniques is being utilized. Current results indicate that vinblastine in the free base form is bound to the protein, but quantitative results are not yet available. These results are consistent with the radioautographic localization of tritiated vinblastine over microtubular crystals in vivo reported by Malawista et al. (16). No bound GTP was detected in the crystals.

DISCUSSION

The similarity in appearance between the crystals formed in vitro by the dialysis of microtubule protein against vinblastine and those formed by the treatment of cells with vinblastine and vincristine is striking. However, it is now apparent, in vitro, that the closely packed arrays of circular profiles are in reality helices viewed on-end, and that the crystal is assembled in much the same manner as a bedspring. The identification of a helical structure suggests that the ladderlike assemblies seen on pelleted and sectioned in vitro material (8) are helices seen in side view. Sectioned crystals, whether produced in vivo or in vitro, have smaller dimensions than those seen in unfixed,
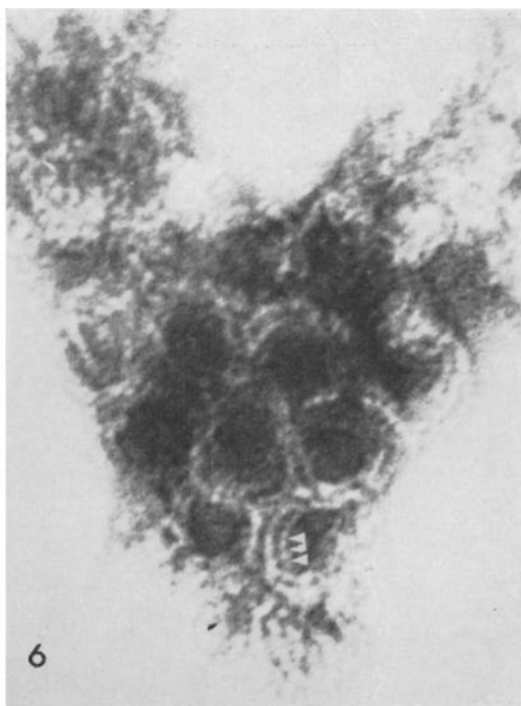
FIGURE 6 Detail of wall structure demonstrating elliptical beaded subunits (arrowheads). Wall width is 80 A and the center-to-center subunit spacing is 50 A. Negative contrast. × 350,000.

negative contrast preparations. Reported inner diameters of the circular elements in sectioned material range from 200 to 260 A (3, 4, 8, 10), compared to 280 A in the negatively stained material. A similar difference exists with regard to the total wall between adjacent elements which measures 80–100 A in sectioned material compared to 140 A in the negatively stained crystals. The reported outer diameter of the sectioned material ranges from 280 to 380 A compared to 420 to 440 A in the crystals described here (3, 8, 10). These differences are probably the result of the dehydration of the sectioned preparations. Dehydration may also account for the fact that the profiles in the negative contrast preparations are circular while in sectioned material they often appear to be hexagonal (3).

The pattern of linearly arranged dots which has been reported in longitudinal sections of in vivo crystals might be the result of a fortuitous section through an array of side-by-side helices along their long axes. This is further supported by the fact that adjacent rows of dots are out of register, as would be required if the section passed through the loops of the helix (3). Alternatively, the dots could represent a section through the tips of the helical turns. In either case the spacing would be of approximately the correct dimension.

High resolution studies of the wall structure reveal a pattern compatible with a linear array of globular subunits. This pattern might also be interpreted as a helical bifilar assembly, though the former explanation is more consistent with established hydrodynamic and chemical data on this protein (9, 11, 12). It is of interest that the subunits appear to be ellipitical or rectangular with their long axes oriented at right angles to the direction of assembly, rather than spherical. This same phenomenon was reported by Ledbetter and Porter (13) in high resolution studies of the subunits in normal microtubules, and it is also apparent in similar work by Phillips (14). It is likely that this asymmetry is due to a heavier deposition of stain along the free inner and outer surfaces of the tubules and of the helical elements and to the less ready access of stain to the surfaces where subunit-subunit contacts are formed. The subunits appear to have a core in which stain is deposited in the negative contrast preparations. Similar conformations have been seen in positively stained sections of microtubules where the core appears electron lucent (13, 14).

Tilney and Porter (15) have reported the formation of abnormally large, 360 A diameter tubules in *Actinosphaerium* in which the normal microtubules have been depolymerized by exposure to cold. These tubules were seen to have cross-striations which ran at 45° angles to the long axis. In view of the work reported here, it is likely that these abnormally large microtubules are actually single helical strands.

SUMMARY

Negative contrast studies have shown the similarity between vinblastine-induced microtubule crystals in vivo and the structures formed by vinblastine-induced self-assembly of microtubule subunits in vitro. These structures are seen to be arrays of helices arranged in a bedspring-like array. The subunits strongly resemble those of the normal microtubule.

REFERENCES

1. WISNIEWSKI, H., M. L. SHELANSKI, and R. D. TERRY. 1968. Effects of mitotic spindle inhibitors on neurotubules and neurofilaments in anterior horn cells. *J. Cell Biol.* **38**:224.

2. BENSCH, K. G., and S. E. MALAWISTA. 1968. Microtubule crystals: A new biophysical phenomenon induced by vinca alkaloids. *Nature (London).* **218**:1176.

3. BENSCH, K. G., and M. E. MALAWISTA. 1969. Microtubular crystals in mammalian cells. *J. Cell Biol.* **40**:95.

4. SCHOCHET, S. S., JR., P. W. LAMPERT, and K. M. EARLE. 1968. Neuronal changes induced by intrathecal vincristine sulfate. *J. Neuropathol. Exp. Neurol.* **27**:645.

5. WEISENBERG, R., and S. TIMASHEFF. 1969. Aggregation of microtubule protein induced by vinblastine. *Biophys. J.* **9**:174A.

6. MARANTZ, R., M. VENTILLA, and M. SHELANSKI. 1969. Vinblastine induced precipitation of microtubule protein. *Science (Washington).* **165**: 498.

7. OLMSTED, J., K. CARLSON, R. KLEBE, F. RUDDLE, and J. ROSENBAUM. *Proc. Nat. Acad. Sci. U.S.A.* In press.

8. BENSCH, K. G., R. MARANTZ, H. WISNIEWSKI, and M. L. SHELANSKI. 1969. Vinca alkaloid induced formation of ordered structures from microtubule protein and from brain extracts. *Science (Washington).* **165**:495.

9. WEISENBERG, R. D., G. G. BORISY, and E. W. TAYLOR. 1968. The colchicine-binding protein of mammalian brain and its relation to microtubules. *Biochemistry.* **7**:4466.

10. SCHLAEPFER, W. 1969. The local effect of vincristine sulfate in peripheral nerve. *Fed. Proc.* **28**:2771.

11. SHELANSKI, M L., and E. W. TAYLOR. 1967. Isolation of a protein subunit from microtubules. *J. Cell Biol.* **34**:549.

12. SHELANSKI, M. L., and E. W. TAYLOR. 1968. Properties of the central pair and outer doublet proteins of sea urchin flagella. *J. Cell Biol.* **38**:304.

13. LEDBETTER, M., and K. R. PORTER. 1964. Morphology of microtubules of plant cells. *Science (Washington).* **144**:872.

14. PHILLIPS, D. M. 1966. Substructure of flagellar tubules. *J. Cell Biol.* **31**:635.

15. TILNEY, L. G., and K. R. PORTER. 1967. Studies on the microtubules in heliozoa. II. The effect of low temperature on these structures in the formation and maintenance of axopodia. *J. Cell Biol.* **34**:327.

16. MALAWISTA, S. E., H. SATO, W. A. CREASEY, and K. G. BENSCH. 1969. Vinblastine produces uniaxial birefringence in starfish oocytes. *Fed. Proc.* **28**:3462A.